The spermidine acetyltransferase SpeG regulates transcription of the small RNA RprA

Linda I. Hu[1,#a¶], Ekaterina V. Filippova[2,#b¶], Joseph Dang[3], Sergii Pshenychnyi[4], Jiapeng Ruan[2,#c], Olga Kiryukhina[2], Wayne F. Anderson[2], Misty L. Kuhn[3], and Alan J. Wolfe[1*]

[1] Department of Microbiology and Immunology, Loyola University Chicago, Health Sciences Division, Stritch School of Medicine, Maywood, IL 60153, USA

[2] Center for Structural Genomics of Infectious Diseases, Northwestern University Feinberg School of Medicine, Department of Biochemistry and Molecular Genetics, Chicago, IL 60611, USA

[3] Department of Chemistry and Biochemistry, San Francisco State University, San Francisco, CA 94132, USA

[4] Recombinant Protein Production Core at Chemistry of Life Processes Institute, Northwestern University, Chicago, IL 60208, USA

[#a] Current address: Department of Microbiology-Immunology, Feinberg School of Medicine, Northwestern University, Chicago, IL 60611, USA

[#b] Current address: Department of Biochemistry and Molecular Biology, Knapp Center for Biomedical Discovery, University of Chicago, Chicago, IL 60637, USA

[#c] Current address: Yale University School of Medicine, Department of Digestive Diseases, New Haven, CT 06510, USA

¶ These authors contributed equally to this work

* Corresponding author

Alan J. Wolfe E-mail: awolfe@luc.edu

Abstract

Spermidine *N*-acetyltransferase (SpeG) acetylates and thus neutralizes toxic polyamines. Studies indicate that SpeG plays an important role in virulence and pathogenicity of many bacteria, which have evolved SpeG-dependent strategies to control polyamine concentrations and survive in their hosts. In *Escherichia coli*, the two-component response regulator RcsB is reported to be subject to N^{ε}-acetylation on several lysine residues, resulting in reduced DNA binding affinity and reduced transcription of the small RNA *rprA*; however, the physiological acetylation mechanism responsible for this behavior has not been fully determined. Here, we performed an acetyltransferase screen and found that SpeG inhibits *rprA* promoter activity in an acetylation-independent manner. Surface plasmon resonance analysis revealed that SpeG can physically interact with the DNA-binding carboxyl domain of RcsB. We hypothesize that SpeG interacts with the DNA-binding domain of RcsB and that this interaction might be responsible for SpeG-dependent inhibition of RcsB-dependent *rprA* transcription. This work provides a model for SpeG as a modulator of *E. coli* transcription through its ability to interact with the transcription factor RcsB. This is the first study to provide evidence that an enzyme involved in polyamine metabolism can influence the function of the global regulator RcsB, which integrates information concerning envelope stresses and central metabolic status to regulate diverse behaviors.

Introduction

SpeG, a member of the Gcn5-related *N*-acetyltransferase (GNAT) family, is a bacterial spermidine *N*-acetyltransferase that acetylates spermidine and spermine. These polyamines are toxic to bacteria at high concentrations and acetylation neutralizes this toxicity [1, 2]. Studies indicate that SpeG plays an important role in virulence and pathogenicity of many bacteria, which have evolved SpeG-dependent strategies to control polyamine concentrations and survive in their hosts [3-6]. Kinetic and structural analyses have demonstrated that SpeG from both *Escherichia coli* and *Vibrio cholerae* can acetylate spermidine [7-9]. These studies also showed that SpeG from *V. cholerae* is an allosteric protein; when spermidine binds to its allosteric site, SpeG exhibits a symmetric closed dodecameric structure [7, 9]. Finally, in the absence of spermidine binding, *V. cholerae* SpeG can adopt a unique asymmetric dodecameric structure with an open conformational state [10].

During the course of this study, we found that SpeG also regulates the small RNA *rprA*, whose transcription strictly requires the phosphorylated isoform of the two-component response regulator RcsB [11, 12]. The canonical two-component signal transduction system is composed of two proteins. The first is a sensor kinase that detects a signal and, in response, autophosphorylates a conserved histidine residue using ATP as the phosphoryl donor. The second is a response regulator that autophosphorylates a conserved aspartate residue using the phosphorylated sensor kinase as the phosphoryl donor [for reviews, see [13-15]]. A more complex variant of the basic two-component system is the phosphorelay,

71 such as the Rcs phosphorelay, which consists of five proteins (RcsC, RcsD, RcsF,
72 IgaA, and RcsB). The first four proteins are involved in controlling the
73 phosphorylation status of the response regulator RcsB in response to diverse
74 extracytoplasmic stimuli. The phosphorylation status of RcsB is set by an ATP-
75 dependent protein-protein interaction chain whose core consists of the cytoplasmic
76 membrane-associated sensor kinase/phosphatase RcsC and its cognate histidine
77 phosphotransferase RcsD [16]. The inner membrane protein IgaA favors RcsC
78 phosphatase activity and thus dephosphorylation of RcsB. Relocation of the outer
79 membrane lipoprotein RcsF to the periplasm favors RcsC kinase activity and thus
80 phosphorylation of RcsB. This occurs when RcsF interacts with the C-terminal
81 periplasmic domain of IgaA. Together, RcsF and IgaA regulate the activities of the
82 Rcs phosphorelay components [17-24]. RcsB also can become phosphorylated in
83 response to central metabolic changes via the central metabolite acetyl phosphate
84 [25]. Both mechanisms (RcsC-dependent and acetyl phosphate-dependent)
85 regulate the phosphorylation status of RcsB and thus both control RcsB-dependent
86 processes, such as desiccation, flagellar biogenesis, capsule biosynthesis, and
87 cell division [16, 25-28].

88 The Rcs phosphorelay is unusual, as the response regulator RcsB can form
89 both a homodimer and a variety of heterodimers. The homodimer activates
90 transcription of *rprA* [11, 12, 29], which encodes the small RNA regulator of the
91 stationary phase sigma factor RpoS, and represses transcription of *flhDC*, which
92 encodes the master regulator of the flagellar regulon [25, 30, 31]. To activate
93 synthesis of the capsular exopolysacchararide colanic acid, RcsB forms a complex

with a partner transcription regulator, RcsA, stabilizing the interaction between RcsB and a specific DNA binding site, the "RcsAB box" [32, 33]. RcsB also can form protein-protein complexes with other partner transcription factors, including GadE, RmpA, MatA, BglJ, and RflM; there is also evidence to suggest an interaction with PhoP [34-39]. Because these protein-protein complexes form in response to a variety of conditions, the Rcs system can mediate diverse responses that contribute to biofilm formation, virulence, motility and antibiotic resistance in pathogens [26-28, 34-36].

Biochemical and mass spectrometry analyses indicate that RcsB can become N^{ε}-lysine acetylated on multiple residues [29, 40-42]. Two mechanisms for N^{ε}-lysine acetylation have been reported. One mechanism involves the direct donation of the acetyl group from acetyl phosphate to a deprotonated lysine ε-amino group [41, 43]. The other mechanism is enzymatic, relying on a lysine acetyltransferase (KAT) to catalyze donation of the acetyl group from acetyl-coenzyme A (acCoA) to the ε-amino group of a lysine residue [44]. All known bacterial KATs are members of the large family of GNATs [29, 40, 44-47].

One of our previous studies suggested that acetylation of RcsB diminished its ability to activate *rprA* transcription in *E. coli* [29]. In an effort to identify a KAT that might be responsible, we first screened 21 known *E. coli* genes that encode or are predicted to encode GNATs, seeking those that inhibited *rprA* transcription. This screen revealed that SpeG could inhibit *rprA* activity; however, we obtained no evidence that SpeG functions as a RcsB lysine N^{ε}-acetyltransferase. Instead, we report here that SpeG can interact with RcsB through the latter's DNA binding

117 domain. Our findings represent the first evidence that the metabolic enzyme SpeG
118 can affect transcription by interacting with the response regulator RcsB.
119

120 Results

121 SpeG regulates *rprA* promoter activity

122 While the GNAT YfiQ (also known as Pka and PatZ) can acetylate RcsB *in vitro*
123 [29, 40], the *yfiQ* mutant does not affect RcsB acetylation [29]. Therefore, we
124 suspected another GNAT was responsible for RcsB acetylation and proceeded to
125 test a series of 21 known or putative GNATs. We overexpressed these GNATs and
126 measured their effect on P*rprA-lacZ*, a transcriptional fusion of the RcsB-
127 dependent *rprA* promoter (P*rprA*) and the *lacZ* gene, which we had integrated as
128 a single copy into the chromosome of BW25113 to generate our reference strain
129 AJW3759 (**Table 1**) [12]. From this preliminary screen, we identified SpeG as an
130 inhibitor of P*rprA* activity. When SpeG was overexpressed from a plasmid in the
131 reference strain, P*rprA* activity was reduced compared to the vector control during
132 late exponential growth and during the transition into early stationary phase (OD >
133 1.0, **Fig 1A**, linear regression analysis t=-2.553, p=0.01472). When *speG* was
134 deleted, P*rprA* activity increased in the isogenic *speG* mutant compared to its wild-
135 type parent (**Fig 1B**, linear regression analysis t=7.750, p= 8.65E-12). Based on
136 these results, we conclude that SpeG inhibits transcription from P*rprA*.

137 **Table 1. Bacterial strains, bacteriophage, plasmids, and primers used in this study.**

Strain, phage, plasmid, or primer	Relevant Characteristic	Source/Reference
Strains		
BW25113	F^- λ- Δ(*araD-araB*)567 Δ(*rhaD-rhaB*)*568* Δ*lacZ4787 rrnB3 rph-1 hsdR514*	[48]
AJW3759	BW25113 λΦ(P*rprA142-lacZ*)	λ: λ*rprA142* → BW25113
AJW4589	AJW3759 Δ*speG*::*FRT*	P1: JW1576 [49] → AJW3759, then removed antibiotic marker
AJW4533	AJW3759 Δ*speE*::*FRT*	P1: JW0117 [49] → AJW3759, then removed antibiotic marker
BL21 (DE3) Magic	Competent cells; a derivative of BL21 cells carrying a plasmid encoding rare tRNAs; Kn^R	[50]
Phage		
λ*rprA142*	*rprA142-lacZ*	[12]
Plasmids		
pCA24n	Control plasmid: Cm^R	[51]
pMCSG7	pET21 derivative for ligation independent cloning; adds N-terminal His tag and TEV cleavage site; Ap^R	[52]
pMCSG53	pET21 derivative for ligation independent cloning; adds N-terminal His tag and TEV cleavage site; Ap^R	[53]
pCA24n-*rcsB*	JW4054; IPTG-inducible His_6-RcsB expression; Cm^R	[51]
pCA24n-*speG*	JW1576; IPTG-inducible His_6-SpeG expression; Cm^R	[51]
pCA24n-*speG*(Y135A)	Site-directed mutagenesis of pCA24n-*speG* to carry an alanine at amino acid 135.	This study
pMCSG7-*rcsB*(NTD)	pMCSG7 expressing His_6-RcsB (residues1-147); Ap^R	This study

pMCSG7-*rcsB*(CTD)	pMCSG7 expressing His_6-RcsB (residues128-216); Ap^R	This study
pMCSG53-*rcsA*	pMCSG53 expressing His_6-RcsA (residues 4-207); Ap^R	[7]
pMCSG7-*speG*	pMCSG7 expressing His_6-SpeG; Ap^R	
Primers (5'-3')		
rcsB(CTD)_F	AAGGAGATATACATATGCATCACCATCACCACCATAAATTCACACCGGAGAGCG	This study
rcsB(CTD)_R	AAGTACAGGTTCTCGGTACCTTATTAGTCTTTGTCCGCCGGAGAC	This study
rcsB(NTD)_F	AAGGAGATATACATATGCACCATCATCACCACCATAACAACATGAACGTTATTATCGCAGATGAC	This study
rcsB(NTD)_R	AAGTACAGGTTCTCGGTACCTTATTAGCCATAGCCGCCTGCAG	This study
SDMspeGY135A	AAAGCCAAGCTTGCGGGCAATGTGAATCGCTTTTTCATTCTCTTTATCA	This study
SDMspeGY135A_as	TGATAAAGAGAATGAAAAAGCGATTCACATTGCCCGCAAGCTTGGCTTT	This study

138

Fig 1. The effect of SpeG on *rprA* promoter activity

A. WT cells carrying the P*rprA-lacZ* fusion (AJW3759) were transformed with either a plasmid that expresses SpeG under the control of an IPTG-inducible promoter (p*speG*; pCA24n-*speG*) or the vector control (VC; pCA24n) and grown in TB7 containing 50 μM IPTG to induce SpeG expression and chloramphenicol to maintain the plasmid. Cell growth and β-galactosidase activity were assayed at various points throughout growth. The values represent average promoter activity with standard deviations of triplicate independent cultures. Linear regression analysis of the experimental group WT/p*speG* on *rprA* promoter activity versus WT/VC was statistically significant (t=-2.553, p=0.01472).

B. WT (AJW3759) and isogenic *speG* (AJW4589) strains were assayed for cell growth in TB7 and β-galactosidase activity. The values represent average promoter activity with standard deviations of five independent WT and *speG* cultures. Linear regression analysis of the experimental group *speG* on *rprA* promoter activity versus WT was statistically significant (t=7.750, p= 8.65E-12).

SpeG does not acetylate RcsB *in vitro*

Since SpeG belongs to the GNAT family of acetyltransferases known to acetylate proteins, we also tested the hypothesis that SpeG regulates *rprA* transcription by acetylating RcsB. To accomplish this, we used an *in vitro* colorimetric enzymatic assay with purified recombinant proteins. This assay measures the formation of product (CoA) indirectly via its reaction with dithionitrobenzoic acid (DTNB) to produce the thioanion product thionitrobenzoate

(TNB^{2-}), which is monitored spectrophotometrically at 415 nm [7, 54]. We compared the acetylation activity of SpeG toward spermidine or RcsB. As predicted, we detected SpeG acetylation activity on spermidine when acCoA was present; however, we observed no change in RcsB acetylation status in the presence of SpeG and acCoA (**Fig 2)**. This result suggests that RcsB is not a substrate for SpeG under the conditions we used to assay acetylation.

Fig 2. *In vitro* acetylation activity of SpeG toward RcsB or spermidine. SpeG was incubated with either spermidine or RcsB in the presence of the acetyl donor acCoA to determine if SpeG uses both spermidine and RcsB as substrates. Control reactions of possible non-enzymatic acetylation of SpeG and RcsB via acCoA were also performed. See Materials and Methods for specific reaction conditions.

Spermidine synthase (SpeE) is not required for SpeG-dependent inhibition of *rprA* transcription

The spermidine synthase SpeE transfers a propylamine from decarboxylated S-adenosylmethionine to putrescine to form spermidine, which is both a substrate and an allosteric activator of SpeG [7]. To explore the role of SpeE/spermidine in SpeG overexpression-inhibited P*rprA* activity, we transformed a mutant that does not synthesize spermidine (*speE*) and its WT parent with either the SpeG overexpression plasmid or its vector control and monitored P*rprA* activity (**Fig 3**). SpeG overexpression resulted in reduced P*rprA* activity in both the parental strain (**Fig 3**, linear regression analysis t=-3.752, p=0.000282) and the *speE* mutant (**Fig**

186 **3**, linear regression analysis t=-3.470, p=0.000745). Furthermore, exposure of the
187 *speE* mutant to exogenous spermidine exerted no effect on P*rprA* activity whether
188 or not SpeG was overexpressed (**S1 Fig**). We conclude that SpeG can inhibit
189 *PrprA* activity regardless of SpeE/spermidine status.
190
191 **Fig 3. The effect of overexpressing SpeG or SpeG(Y135A) in WT cells and**
192 **overexpressing SpeG in the *speE* mutant on *rprA* promoter activity**
193 A. WT cells carrying the P*rprA-lacZ* fusion (AJW3759) were transformed with
194 either p*speG* (pCA24n-*speG*), p*speG(Y135A)* (pCA24n-*speG(Y135A)*), or the VC
195 (pCA24n) and grown in TB7 supplemented with 50 μM IPTG and
196 chloramphenicol to maintain the plasmid. Cell growth and β-galactosidase activity
197 were assayed. The values represent average promoter activity with standard
198 deviations of five independent cultures.
199 B. The isogenic *speE* mutant was transformed with either p*speG* (pCA24n-*speG*)
200 or the VC (pCA24n) and cell growth and β-galactosidase activity were assayed as
201 described for 3A. The values represent average promoter activity with standard
202 deviations of five independent cultures. Linear regression comparison results on
203 *rprA* promoter activity were significant for all experimental groups: WT/p*speG*
204 versus WT/VC (t=-3.752, p=0.000282), WT/p*speG(Y135A)* versus WT/VC
205 (t= -2.456, p=0.015623), and *speE*/p*speG* versus *speE*/VC (t=-3.470,
206 p=0.000745).
207
208

209 **Catalytic activity of SpeG is not required for SpeG-dependent inhibition of**
210 ***rprA* transcription**

211 We next asked if SpeG overexpression-dependent inhibition of P*rprA* activity
212 requires the spermidine acetyltransferase activity of SpeG. We therefore
213 overexpressed SpeG Y135A, a predicted catalytically inactive SpeG variant, in the
214 parent (AJW3759). This tyrosine (Y) residue acts as a general acid during
215 substrate acetylation and has been shown to be critical for catalytic activity of many
216 GNAT homologs [55-57]. We found that the SpeG Y135A mutant retained the
217 ability to inhibit P*rprA* activity in the parent AJW3759 (**Fig 3A**, linear regression
218 analysis t= -2.456, p=0.015623). These results are consistent with a SpeG-
219 dependent, but spermidine acetylation-independent mechanism of inhibition in WT
220 cells.

221

222 **SpeG binds to RcsB through its C-terminal domain**

223 Since SpeG does not appear to acetylate RcsB and its catalytic activity is
224 unnecessary for its ability to inhibit *rprA* transcription, we considered whether
225 SpeG inhibits RcsB activity through a physical interaction. We used SPR to
226 investigate whether SpeG and RcsB can form a complex. First, we immobilized
227 SpeG onto the SPR chip and evaluated whether full-length RcsB or its N- or C-
228 terminal domains could bind to SpeG. Both full-length RcsB (**Fig 4A**) and its C-
229 terminal domain (**Fig 4B**) bound to immobilized SpeG in a concentration-
230 dependent manner. In contrast, the N-terminal domain of RcsB did not (**Fig 4C**).
231 These results suggest that RcsB binds to SpeG through its C-terminal domain. We

232 also performed the reverse experiment, assessing whether SpeG could bind to
233 immobilized RcsB or its domains, but we detected no signal (data not shown).
234 Perhaps RcsB binds to the chip in a manner that prevents interaction with SpeG.
235
236 **Fig 4. SPR analysis of the SpeG-RcsB interaction**
237 The dose-response analysis for immobilized *E. coli* SpeG (46 μM) with increasing
238 concentrations of full-length *E. coli* RcsB (21, 42, 53, 63 and 74 μM) as an analyte
239 in the absence of spermidine (A) or RcsB (21, 42, 53, 63 and 74 μM) after exposure
240 to 0.5 mM spermidine (D), RcsB C-terminal domain (45, 67, 91, 114, 136, and 159
241 μM) in the absence of spermidine (B) or RcsB C-terminal domain (23, 45, 91, 114,
242 and 136 μM) after exposure to 0.5 mM spermidine (E), and RcsB N-terminal
243 domain (59, 118, and 176 μM) in the absence of spermidine (C) or RcsB N-terminal
244 domain (59, 118, 177, 236 and 295 μM) after exposure to 0.5 mM spermidine (F).
245
246 We calculated a K_D of 67 μM for the binding of SpeG to the RcsB C-terminal
247 domain from the fit to a simple one-to-one binding model, in which one C-domain
248 RcsB molecule interacts with one SpeG molecule (**S2A Fig**). However, we could
249 not determine the K_D for the SpeG/full-length RcsB interaction, as the data did not
250 fit either a simple binding model or other models defined in the SPR data analysis
251 software program TraceDrawer. The lack of fitting for the SpeG/full-length RcsB
252 interaction likely resulted from the pronounced peak at the beginning of the
253 sensograms, which occurred especially with higher concentrations of RcsB.

We next tested the effect of spermidine on the SpeG-RcsB interaction. To accomplish this, we exposed the surface of the chip containing immobilized SpeG to spermidine and then measured the SPR signal from binding the three separate RcsB constructs (described in Materials and Methods; **Fig 4D-F**). By fitting the sensograms to these data using the one-to-one binding model, we obtained K_D values of 128 and 281 μM for the RcsB full-length and its C-terminal domain, respectively (**Fig S2B-C**). In contrast, we could not determine a K_D for the RcsB N-terminal domain due to a large chi-squared fitting value. Furthermore, we conclude that the binding of the N-terminal domain to SpeG is weak because the response signals obtained at concentrations greater than 100 μM were relatively low (**Fig 4F**). On the basis of these data and those obtained in the absence of spermidine, we propose that SpeG interacts with the C-terminal domain of RcsB in the presence or absence of spermidine and that spermidine does not prevent RcsB binding to SpeG.

Possible SpeG inhibition of LuxR/FixJ-like transcription factors

SpeG inhibits *rprA* transcription and binds RcsB through the carboxyl terminal domain, which contains the conserved DNA binding helix-turn-helix (HTH) motif found in RcsB and other LuxR/FixJ-type proteins [16, 58]. Based on this result, it is tempting to speculate that SpeG may also bind other LuxR/FixJ family members. To identify conserved residues of the RcsB HTH motif across other LuxR/FixJ-like transcriptional regulators from *E. coli*, we used the PSI-BLAST server [59] to generate a list of DNA-binding domains from LuxR/FixJ-type family homologs and

277 the NMR structure of the RcsB C-terminal domain from *Erwinia amylovora,* a close
278 relative of *E. coli* [32] to visualize sequence conservation with respect to the three-
279 dimensional structure (**Fig 5**). We also generated a phylogenetic tree using these
280 sequences to determine which RcsB homologs had the greatest sequence
281 similarity to its C-terminal domain and, therefore, propensity for interacting with
282 SpeG (**S3 Fig**). We found the most conserved RcsB C-terminal domain residues
283 across LuxR/FixJ-type homologs are S152, P153, K154, L167, V168, T169, R177,
284 S178, K180, T181, S183, S184, Q185, K186, K187, and D198. From our analysis,
285 the *E. coli* LuxR/FixJ-type homolog sequences of YjjQ, BglJ, YahA, YuaB, DctR,
286 and RcsA are most similar to the RcsB C-terminal DNA-binding domain and
287 warrant further testing. We hypothesized that SpeG might bind RcsB through these
288 critical residues in the C-terminal domain and potentially those of other homologs.
289

290 **Fig 5. Structure analysis of the RcsB C-terminal DNA-binding domain**
291 Ribbon diagram of the RcsB C-terminal DNA-binding domain from *Erwinia*
292 *amylovora* (top panel). Conserved residues involve in DNA contacts in known
293 LuxR/FixJ regulators are shown as stick models. RcsB DNA-binding domain:
294 sequence-structure alignment (bottom panel). Surface representation of the RcsB
295 DNA-binding domain was colored by the degree of sequence conservation from
296 red (100% conserved residues) to blue (non-conserved residues). A search for
297 RcsB C-terminal DNA-binding domain homologs was done using the PSI-BLAST
298 server. From the list of 500 sequences against the non-redundant database a
299 random set of 30 sequences with identity from 98% to 40% were chosen. A multiple

sequence alignment for visualization of the sequence conservation with respect to the three-dimensional structure was generated.

SpeG does not bind the LuxR/FixJ family member RcsA

To determine if binding to SpeG is specific for RcsB or if SpeG can bind *in vitro* to other LuxR/FixJ transcriptional regulators that have C-terminal domains similar to RcsB, we heterologously expressed and purified the *E. coli* RcsA transcriptional regulator (an auxiliary partner with RcsB in a heterodimer that interacts with a specific DNA site called the “RcsAB” box [60]) and tested RcsA binding to SpeG by SPR. We found that SpeG does not bind to RcsA in the absence of spermidine (**S4 Fig**), which highlights the binding specificity between RcsB and SpeG. However, we cannot exclude that possibility that SpeG may bind an RcsB-RcsA heterodimer or other LuxR/FixJ-type family members in the presence or absence of spermidine. While RcsA has an HTH motif, its inability to bind SpeG also suggests that other regions of RcsB within its DNA-binding domain besides the HTH motif and/or its oligomeric state might be important for the specificity of the SpeG-RcsB interaction.

Discussion

We have presented evidence that the metabolic enzyme SpeG regulates transcription from the *rprA* promoter. We also have shown that SpeG binds the DNA binding domain of the transcription factor RcsB. We propose that this interaction interferes with the ability of RcsB to activate transcription from the *rprA*

323 promoter. This represents the first report of a direct link between spermidine
324 metabolism and an envelope stress signal transduction pathway.
325
326 **SpeG can inhibit *rprA* transcription through interactions with RcsB**
327 We began this study because we had previously reported that N$^{\varepsilon}$-lysine
328 acetylation regulates RcsB activity at the *rprA* promoter [29]. Since deletion of the
329 only known *E. coli* N$^{\varepsilon}$-lysine acetyltransferase YfiQ had no obvious effect on the
330 acetylation state of RcsB [29], we screened the known and putative
331 acetyltransferases for regulators of *rprA* transcription and found that SpeG
332 inhibited *rprA* promoter activity: overexpression of SpeG reduced *rprA* promoter
333 activity (**Fig 1A**), while deleting *speG* relieved inhibition of the *rprA* promoter (**Fig**
334 **1B**).
335 Because we did not observe acetylation of RcsB by SpeG (**Fig 2**) and since we
336 did not find that SpeG activity could affect RcsB-dependent *rprA* inhibition (**Fig 3**),
337 we instead investigated the possibility of a physical interaction between RcsB and
338 SpeG. Indeed, SPR analysis showed that SpeG forms a complex with RcsB
339 through the RcsB C-terminal DNA-binding domain (**Fig 4**). We further report that
340 this interaction is specific, as we did not detect binding between SpeG and RcsB's
341 auxiliary transcription factor RcsA (57) (**S3 and S4 Figs**). These *in vitro* results
342 combined with the *in vivo* analysis support the hypothesis that SpeG and RcsB
343 interact and that the resulting complex impacts RcsB activity at the *rprA* promoter.
344 As *rprA* transcription absolutely requires RcsB, we did not test if SpeG affected
345 *rprA* transcription in an *rcsB* mutant.

346

347 **Physiological implications of SpeG-RcsB interactions**

348 It has been estimated that RcsB regulates 5% of the *E. coli* genome,
349 including but not limited to the colanic acid biosynthetic locus, the small RNA *rprA*,
350 and the operon that encodes FlhDC, the master regulator of flagellar biogenesis
351 [61, 62]. The Rcs phosphorelay has also been implicated in regulating biofilm
352 formation and sensitivity to antibiotic-induced peptidoglycan damage [16, 62-64].
353 Since the SpeG interaction with RcsB regulates activation of *rprA* transcription,
354 SpeG likely influences these other RcsB-regulated phenotypes. In fact, it has been
355 reported that polyamines can induce the glutamate-dependent acid response
356 system [65], which requires RcsB [66]. The outstanding question is why polyamine
357 neutralization and cellular processes regulated by RcsB would be coordinated. We
358 conjecture that SpeG works through members of the RcsB regulon required to
359 initiate proper responses to particular extracellular conditions such as cold shock,
360 heat shock, ethanol, and increased alkalinity, which were shown to influence the
361 spermidine metabolic pathway [67].

362

363 Conclusion

364 We have shown that SpeG and RcsB can form a complex, suggesting a
365 coordinated response between polyamine metabolism and envelope stress. It is
366 not known why an enzyme involved in spermidine metabolism regulates RcsB, if
367 RcsB affects spermidine biosynthesis, or whether SpeG acts as a general
368 modulator of response regulators. However, it is clear that SpeG inhibits RcsB

activity *in vivo* and we propose that it is through a direct interaction between SpeG and the DNA binding domain of RcsB.

Materials and Methods

Bacterial strains, bacteriophage, and plasmids

All of the bacterial strains, bacteriophage, and plasmids used in this study are listed in **Table 1**. Derivatives were constructed by generalized transduction with P1kc [68]. P*rprA142-lacZ*, a transcriptional fusion of the *rprA* promoter (*PrprA*) to the *lacZ* reporter, was from Dr. Susan Gottesman (National Institutes of Health, Bethesda, MD) [12]. Construction of monolysogens was performed and verified as described previously [69]. Transformations were performed by electroporation or through the use of either transformation buffers 1 and 2 [70] or transformation-and-storage solution [71].

Culture conditions

For strain construction, cells were grown in lysogeny broth (LB) consisting of 1% (w/v) tryptone, 0.5% (w/v) yeast extract, and 0.5% (w/v) sodium chloride; LB plates contained 1.5% agar. For promoter activity assays, cells were grown in tryptone broth buffered at pH 7 (TB7), which contains 1% (w/v) tryptone buffered at pH 7.0 with potassium phosphate (100 mM). Cell growth was monitored spectrophotometrically (DU640; Beckman Instruments, Fullerton, CA) by determining the absorbance at 600 nm (OD_{600}). Chloramphenicol (25 µg/ml) was added to growth media when needed to maintain pCA24n plasmid derivatives. To

392 induce the expression of genes carried on various plasmids, 10 μM isopropyl-β-D-
393 thiogalactopyranoside (IPTG) was added to the growth media.
394
395 **β-galactosidase assay**
396 To monitor the promoter activity of P*rprA-lacZ*, biological replicates were grown
397 aerobically at 37°C in TB7 overnight. The overnight cultures were diluted in fresh
398 TB7 to an OD_{600} of 0.05 and grown aerobically with agitation at 250 rpm at 37°C
399 until early stationary phase. At regular intervals, cells were harvested and stored
400 at 4°C in a microtiter plate. β-galactosidase activity was determined quantitatively
401 as described previously (26) using All-in-One β-galactosidase reagent (Pierce
402 Biochemical). Sterile TB7 was used as a negative control on each microtiter plate.
403 Promoter activity was monitored throughout growth and plotted against OD_{600}.
404 Each individual experiment included at least three biological replicates. Each of
405 these experiments was performed at least three times. The values represent the
406 means with standard deviations.
407
408 **Site-directed mutagenesis**
409 Site-directed mutagenesis of SpeG to pCA24n-speG(Y135A) was conducted
410 in pCA24n-*speG* with the QuikChange Lightning Multi site-directed mutagenesis
411 kit (Agilent Technologies), in accordance with the manufacturer's instructions by
412 using the mutagenic primers SDMspeGY135A and SDMspeGY135A_as, as listed
413 in **Table 1**.
414

415 **RcsB, RcsA and SpeG expression plasmids**

416 Plasmids containing genes from *Escherichia coli* str. K-12 substr. MG1655
417 included the following: 1) full-length RcsB (NCBI accession code AAC75277, GI:
418 1788546) in the pCA24n vector from the ASKA collection (chloramphenicol
419 resistant; pCA24n-*rcsB*) [51], 2) the N-terminal receiver domain of RcsB (truncated
420 construct, residues 1-147) in the pMCSG7 vector (ampicillin resistant; pMCSG7-
421 *rcsB*(NTD)), 3) the C-terminal DNA binding domain of RcsB (truncated construct,
422 residues 128-216) in the pMCSG7 vector (ampicillin resistant; pMCSG7-
423 *rcsB*(CTD)), 4) full-length RcsA (NCBI accession code WP_000104001 and GI:
424 CTS77413) in the pMCSG53 vector (ampicillin resistant; pMCSG53-*rcsA*) and 5)
425 full-length SpeG (NCBI accession code NP_416101, GI: 16129542) in the
426 pMCSG7 vector (ampicillin resistant; pMCSG7-*speG*). The full-length RcsB
427 construct (pCA24n-*rcsB*) and its truncated versions ((pMCSG7-*rcsB*(NTD) and
428 pMCSG7-*rcsB*(CTD)) had an uncleavable N-terminal polyhistidine tag, while the
429 RcsA (pMCSG53-*rcsA*) and SpeG (pMCSG7-*speG*) constructs had a cleavable N-
430 terminal polyhistidine tag followed by a TEV protease cleavage site [51]. The
431 genes for the individual RcsB domains were synthesized by Genescript and
432 subcloned into the pMCSG7 vector using ligation independent cloning as
433 described previously [72, 73]. A portion of the linker sequence (comprised of
434 residues 121-149) between the domains was included in each individual domain
435 construct.

436

437 **Large-scale protein expression and purification**

438 Expression plasmids containing the desired genes were transformed into
439 kanamycin-resistant BL21(DE3)-magic or KRX/pGro7 (for pMCSG53-*rcsA*)
440 competent cells [74]. pCA24n-*rcsB* transformants were grown in Terrific Broth (TB)
441 in the presence of 34 µg/mL chloramphenicol and 35 µg/mL kanamycin. pMCSG7-
442 *rcsB*(NTD) and pMCSG7-*rcsB*(CTD) transformants were grown in LB in the
443 presence of 400 µg/mL ampicillin and 25 µg/mL kanamycin. The pMCSG53-*rcsA*
444 transformant was grown in M9 L-selenomethionine supplemented media
445 (Medicilon Inc.) in the presence of 400 µg/mL ampicillin, 35 µg/mL kanamycin and
446 0.1% arabinose. pMCSG7-*speG* transformants were grown in TB supplemented
447 with 100 µg/mL ampicillin and 50 µg/mL kanamycin.

448 Full-length RcsB protein, its N-terminal and C-terminal domains, and RcsA
449 protein were prepared at the Recombinant Protein Production Core (rPPC) Facility
450 at Northwestern University (Evanston, IL, USA). Transformants containing the
451 RcsB and RcsA plasmids were grown at 37°C in a fermenter until the OD_{600}
452 reached 0.8, whereupon they were induced with 0.6 mM IPTG. The RcsA
453 transformant was also exposed to 0.25% L-rhamnose. The RcsB constructs were
454 expressed at 25°C overnight, whereas RcsA was expressed at 22°C overnight.
455 The next day cells were harvested by centrifugation and resuspended in lysis
456 buffer (1.5 mM magnesium acetate, 1mM calcium chloride, 250 mM sodium
457 chloride, 100 mM ammonium sulfate, 40 mM disodium phosphate, 3.25 mM citric
458 acid, 5% glycerol, 5 mM imidazole, 5 mM beta-mercaptoethanol (BME), 0.08% n-
459 dodecyl-beta-maltoside (DDM), 1 mM phenylmethylsulfonyl fluoride (PMSF), and
460 20 µM leupeptin) and homogenized. Cells containing the SpeG plasmid were

461 grown at 37°C in a benchtop shaker to an OD_{600} of 0.6, induced with 0.5 mM IPTG,
462 and expressed at 25°C overnight. Cells were harvested and resuspended in lysis
463 buffer (as stated above without PMSF and leupeptin) and sonicated. After
464 sonication, lysates were centrifuged and the supernatant was purified as follows.

465 The proteins were purified using an ÄKTAxpress™ (GE Healthcare,
466 Piscataway, NJ) high-throughput purification system at 4°C. The crude extract was
467 loaded onto a 5 mL HisTrap FF Ni-NTA column, washed with loading buffer (10
468 mM Tris HCl pH 8.3, 500 mM sodium chloride and 5 mM BME), washed with
469 loading buffer plus 25 mM imidazole to remove impurities, and eluted with loading
470 buffer plus 500 mM imidazole. The purified proteins were subsequently loaded
471 onto and eluted from a HiLoad™ 26/60 Superdex™ 200 size-exclusion column in
472 loading buffer. The polyhistidine tag of the SpeG protein was removed, as
473 described previously [75]; for all other constructs, the tag remained attached. The
474 final purity of each protein was assayed by SDS-PAGE.

475

476 **Enzyme kinetic assays**

477 To test whether SpeG could acetylate RcsB, we performed *in vitro* enzyme
478 kinetics, using a previously described assay and recombinantly expressed and
479 purified proteins [7, 54]. The total volume for each reaction was 50 µL and
480 contained 50 mM Bicine pH 9.0, 0.5 mM acCoA, 1 mM spermidine, 0.96 µM SpeG
481 enzyme, and/or 0.1 mM RcsB full-length protein. All reactions were initiated with
482 10 µL of SpeG enzyme or enzyme dilution buffer (100 mM Bicine pH 9.0, 100 mM
483 sodium chloride) and were performed in triplicate at 35°C for 20 min. To stop the

484 reactions, 50 µL of a solution containing 100 mM Tris HCl pH 8.0 and 6 M
485 guanidine HCl was added to each reaction. To detect the product of the reaction
486 (CoA), 200 µL of a solution containing 0.2 m*M* 5,5′-Dithiobis(2-nitrobenzoic acid),
487 100 m*M* Tris HCl pH 8.0, and 1 mM EDTA was added to each reaction and
488 incubated for 10 min at room temperature. The absorbance was then measured at
489 415 nm on a Biotek ELx808 microplate reader.
490
491 **Surface plasmon resonance (SPR) analysis of binding interactions between**
492 **SpeG and RcsB in absence or presence of spermidine**
493 Binding interactions of *E. coli* SpeG to full-length *E. coli* RcsB or individual RcsB
494 domains in the absence of spermidine were measured using a Reichert
495 SR7500DC (Reichert Technologies, Buffalo, NY) dual channel spectrometer at the
496 Keck Biophysics Facility at Northwestern University (Evanston IL, USA). Prior to
497 immobilizing SpeG onto a carboxymethyl dextran hydrogel surface gold sensor
498 chip (Reichert Technologies, Buffalo, NY), the surface of the chip containing COO^-
499 groups were activated with a mixture of N-hydroxysuccinimide (NHS) and 1-ethyl-
500 3-(3-dimethylaminopropyl)carbodiimide hydrochloride (EDC) to create amine
501 reactive esters. SpeG protein (46 µM) in solution containing 10 mM HEPES at pH
502 8.3 and 100 mM sodium chloride was then immobilized onto the chip and
503 covalently coupled with the surface NHS esters at a flow rate of 40 µL/min at room
504 temperature. To achieve saturation, two sequential injections of SpeG for 3 min
505 followed by 1.5 min of dissociation were performed. To block formation of residual
506 NHS esters, an ethanolamine solution was injected over the chip. To remove

weakly bound SpeG molecules, the chip was washed with running buffer containing 10 mM HEPES at pH 8.3 and 100 mM sodium chloride. The instrument was cooled and all SPR measurements were carried out at 4°C. All protein solutions were prepared in running buffer. 160 µL of RcsB full-length (10, 21, 42, 53, 63 and 74 µM), RcsB C-terminal domain (45, 67, 91, 114, 136, and 159 µM), or RcsB N-terminal domain (59, 118, and 176 µM) were injected sequentially over the SpeG-chip with a flow rate of 40 µL min^{-1} for 30 sec followed by a 1.5 min rinse and a 1 min dissociation. After each binding cycle, SpeG surfaces were regenerated by injecting 0.5 M sodium chloride for 45 sec at a flow rate of 30 µL min^{-1} and washed with running buffer. All analyte injections were performed in duplicate. For each measurement, a background response recorded in the reference cell was subtracted as well as the response from a blank injection with the running buffer.

To investigate how spermidine affects binding interactions of SpeG to RcsB and its individual domains, we used a Reichert4SR (Reichert Technologies, Buffalo, NY) four-channel SPR system at the Keck Biophysics Facility. SpeG was immobilized at a concentration of 46 µM onto cells 3 and 4 using the amine coupling procedure described above. Cells 1 and 2 were used as reference cells. All measurements were performed at 4°C. A solution containing 0.5 mM spermidine in the running buffer was flowed over the surface of the immobilized SpeG at 40 µL min^{-1} for 30 sec followed by a 1.5 min rinse and a 1 min dissociation. The chip was then washed with running buffer until the SPR signal reached a stable value. 160 µL of RcsB full-length (10, 21, 42, 53, 63 and 74 µM), RcsB C-

terminal domain (23, 45, 91, 114, and 136 μM) or RcsB N-terminal domain (59, 118, 177, 236 and 295 μM) were injected sequentially over the SpeG-chip, as described above, to monitor binding of RcsB constructs to SpeG in the presence of spermidine. After each binding cycle of RcsB full-length and RcsB C-terminal domain, SpeG surfaces were regenerated with an injection of 0.5 M sodium chloride for 1.5 min at a flow rate of 30 μL min^{-1} and washed with the running buffer. Regeneration of the chip surface after injections of RcsB N-terminal domain was not required because the protein dissociated on its own. A background response for each run and the response from a blank injection were subtracted. With the exception of the RcsB N-terminal domain in the absence of spermidine, duplicate measurements were collected for each concentration of each protein. Data processing and kinetic analyses for all experiments were performed using TraceDrawer Data Analysis software (Reichert Technologies, Buffalo, NY).

SPR analysis of binding interactions between SpeG and the transcription factor RcsA

To examine binding interactions between SpeG and RcsB's auxiliary partner RcsA from *E. coli*, we used a four-channel SPR system at the Keck Biophysics Facility following the amine coupling protocol, as described above. SpeG protein at a concentration of 46 μM in 10 mM HEPES buffer at pH 8.3 containing 100 mM sodium chloride was immobilized onto the chip. 160 μL of RcsA protein solution in running buffer (21, 42, 64 and 85 μM) was injected consecutively over the SpeG-chip followed by regeneration and washing, as described above. A background

553 response and response from a blank injection that contained running buffer were
554 subtracted from each sensorgram to determine the actual binding response. Data
555 were processed using TraceDrawer software.
556
557 **Linear Regression Analysis**
558 To determine whether experimental results were statistically significant, a linear
559 regression was performed, comparing all experimental groups with their respective
560 vector controls. All of the regressions used were set up as follows: the calculated
561 *rprA* promoter activity was the response variable, the overexpressed plasmids or
562 mutant were the explanatory variable, and time was a random effect. OD was not
563 included as an effect on activity as it is already used in the calculation of activity.
564 Time as a random effect was chosen based on the question asked: Accounting for
565 the effects of time on activity does the experimental group in question significantly
566 affect overall *rprA* promoter activity? The significance threshold was set at 0.05.
567 The open source program R (version 3.3.2) and packages “lmerTest”, “ggplot2”,
568 and “moments” were used to visualize and analyze the data (76,77,78,79).
569

570 # Acknowledgements

571 We would like to thank the Keck Biophysics Facility at Northwestern
572 University (Evanston, IL) for assistance with SPR data collection, Roberto Limeira
573 and Cara Joyce (Loyola University Chicago) for the linear regression analyses of
574 the *in vivo* data, Sarah Cook, David Christensen, and Bozena Zemaitaitis (Loyola
575 University Chicago) for helping to complete and repeat the acetyltransferase

576 overexpression experiments, and the members of the Visick and Wolfe labs
577 (Loyola University Chicago) for important scientific discussions pertaining to this
578 study.

579

References

1. Fukuchi J, Kashiwagi K, Yamagishi M, Ishihama A, Igarashi K. Decrease in cell viability due to the accumulation of spermidine in spermidine acetyltransferase-deficient mutant of Escherichia coli. The Journal of biological chemistry. 1995;270(32):18831-5.
2. Limsuwun K, Jones PG. Spermidine acetyltransferase is required to prevent spermidine toxicity at low temperatures in Escherichia coli. Journal of bacteriology. 2000;182(19):5373-80.
3. Barbagallo M, Di Martino ML, Marcocci L, Pietrangeli P, De Carolis E, Casalino M, et al. A new piece of the Shigella Pathogenicity puzzle: spermidine accumulation by silencing of the speG gene [corrected]. PloS one. 2011;6(11):e27226.
4. Campilongo R, Di Martino ML, Marcocci L, Pietrangeli P, Leuzzi A, Grossi M, et al. Molecular and functional profiling of the polyamine content in enteroinvasive E. coli : looking into the gap between commensal E. coli and harmful Shigella. PloS one. 2014;9(9):e106589.
5. Joshi GS, Spontak JS, Klapper DG, Richardson AR. Arginine catabolic mobile element encoded speG abrogates the unique hypersensitivity of Staphylococcus aureus to exogenous polyamines. Molecular microbiology. 2011;82(1):9-20.
6. Thurlow LR, Joshi GS, Clark JR, Spontak JS, Neely CJ, Maile R, et al. Functional modularity of the arginine catabolic mobile element contributes to the success of USA300 methicillin-resistant Staphylococcus aureus. Cell host & microbe. 2013;13(1):100-7.
7. Filippova EV, Kuhn ML, Osipiuk J, Kiryukhina O, Joachimiak A, Ballicora MA, et al. A novel polyamine allosteric site of SpeG from Vibrio cholerae is revealed by its dodecameric structure. Journal of molecular biology. 2015;427(6 Pt B):1316-34.
8. Fukuchi J, Kashiwagi K, Takio K, Igarashi K. Properties and structure of spermidine acetyltransferase in Escherichia coli. The Journal of biological chemistry. 1994;269(36):22581-5.
9. Sugiyama S, Ishikawa S, Tomitori H, Niiyama M, Hirose M, Miyazaki Y, et al. Molecular mechanism underlying promiscuous polyamine recognition by spermidine acetyltransferase. The international journal of biochemistry & cell biology. 2016;76:87-97.
10. Filippova EV, Weigand S, Osipiuk J, Kiryukhina O, Joachimiak A, Anderson WF. Substrate-Induced Allosteric Change in the Quaternary Structure of the Spermidine N-Acetyltransferase SpeG. Journal of molecular biology. 2015;427(22):3538-53.
11. Majdalani N, Chen S, Murrow J, St John K, Gottesman S. Regulation of RpoS by a novel small RNA: the characterization of RprA. Molecular microbiology. 2001;39(5):1382-94.
12. Majdalani N, Hernandez D, Gottesman S. Regulation and mode of action of the second small RNA activator of RpoS translation, RprA. Molecular microbiology. 2002;46(3):813-26.
13. Bourret RB. Receiver domain structure and function in response regulator proteins. Current opinion in microbiology. 2010;13(2):142-9.

623 14. Salazar ME, Laub MT. Temporal and evolutionary dynamics of two-component
624 signaling pathways. Current opinion in microbiology. 2015;24:7-14.
625 15. Jung K, Fried L, Behr S, Heermann R. Histidine kinases and response regulators
626 in networks. Current opinion in microbiology. 2012;15(2):118-24.
627 16. Majdalani N, Gottesman S. The Rcs phosphorelay: a complex signal
628 transduction system. Annual review of microbiology. 2005;59:379-405.
629 17. Mariscotti JF, Garcia-Del Portillo F. Instability of the Salmonella RcsCDB
630 signalling system in the absence of the attenuator IgaA. Microbiology. 2008;154(Pt
631 5):1372-83.
632 18. Castanie-Cornet MP, Cam K, Jacq A. RcsF is an outer membrane lipoprotein
633 involved in the RcsCDB phosphorelay signaling pathway in Escherichia coli. Journal
634 of bacteriology. 2006;188(12):4264-70.
635 19. Cho SH, Szewczyk J, Pesavento C, Zietek M, Banzhaf M, Roszczenko P, et al.
636 Detecting envelope stress by monitoring beta-barrel assembly. Cell.
637 2014;159(7):1652-64.
638 20. Konovalova A, Perlman DH, Cowles CE, Silhavy TJ. Transmembrane domain of
639 surface-exposed outer membrane lipoprotein RcsF is threaded through the lumen of
640 beta-barrel proteins. Proceedings of the National Academy of Sciences of the United
641 States of America. 2014;111(41):E4350-8.
642 21. Mariscotti JF, Garcia-del Portillo F. Genome expression analyses revealing the
643 modulation of the Salmonella Rcs regulon by the attenuator IgaA. Journal of
644 bacteriology. 2009;191(6):1855-67.
645 22. Hussein NA, Cho SH, Laloux G, Siam R, Collet JF. Distinct domains of Escherichia
646 coli IgaA connect envelope stress sensing and down-regulation of the Rcs
647 phosphorelay across subcellular compartments. PLoS Genet. 2018;14(5):e1007398.
648 23. Pucciarelli MG, Rodriguez L, Garcia-Del Portillo F. A Disulfide Bond in the
649 Membrane Protein IgaA Is Essential for Repression of the RcsCDB System. Front
650 Microbiol. 2017;8:2605.
651 24. Sato T, Takano A, Hori N, Izawa T, Eda T, Sato K, et al. Role of the inner-
652 membrane histidine kinase RcsC and outer-membrane lipoprotein RcsF in the
653 activation of the Rcs phosphorelay signal transduction system in Escherichia coli.
654 Microbiology. 2017;163(7):1071-80.
655 25. Fredericks CE, Shibata S, Aizawa S, Reimann SA, Wolfe AJ. Acetyl phosphate-
656 sensitive regulation of flagellar biogenesis and capsular biosynthesis depends on the
657 Rcs phosphorelay. Molecular microbiology. 2006;61(3):734-47.
658 26. Howery KE, Clemmer KM, Rather PN. The Rcs regulon in Proteus mirabilis:
659 implications for motility, biofilm formation, and virulence. Current genetics. 2016.
660 27. Lehti TA, Heikkinen J, Korhonen TK, Westerlund-Wikstrom B. The response
661 regulator RcsB activates expression of Mat fimbriae in meningitic Escherichia coli.
662 Journal of bacteriology. 2012;194(13):3475-85.
663 28. Wang Q, Harshey RM. Rcs signalling-activated transcription of rcsA induces
664 strong anti-sense transcription of upstream fliPQR flagellar genes from a weak
665 intergenic promoter: regulatory roles for the anti-sense transcript in virulence and
666 motility. Molecular microbiology. 2009;74(1):71-84.

667 29. Hu LI, Chi BK, Kuhn ML, Filippova EV, Walker-Peddakotla AJ, Basell K, et al.
668 Acetylation of the response regulator RcsB controls transcription from a small RNA
669 promoter. Journal of bacteriology. 2013;195(18):4174-86.
670 30. Francez-Charlot A, Laugel B, Van Gemert A, Dubarry N, Wiorowski F, Castanie-
671 Cornet MP, et al. RcsCDB His-Asp phosphorelay system negatively regulates the flhDC
672 operon in Escherichia coli. Molecular microbiology. 2003;49(3):823-32.
673 31. Filippova EV, Zemaitaitis B, Aung T, Wolfe AJ, Anderson WF. Structural Basis
674 for DNA Recognition by the Two-Component Response Regulator RcsB. MBio.
675 2018;9(1).
676 32. Pristovsek P, Sengupta K, Lohr F, Schafer B, von Trebra MW, Ruterjans H, et al.
677 Structural analysis of the DNA-binding domain of the Erwinia amylovora RcsB protein
678 and its interaction with the RcsAB box. The Journal of biological chemistry.
679 2003;278(20):17752-9.
680 33. Wehland M, Bernhard F. The RcsAB box. Characterization of a new operator
681 essential for the regulation of exopolysaccharide biosynthesis in enteric bacteria. The
682 Journal of biological chemistry. 2000;275(10):7013-20.
683 34. Castanie-Cornet MP, Cam K, Bastiat B, Cros A, Bordes P, Gutierrez C. Acid stress
684 response in Escherichia coli: mechanism of regulation of gadA transcription by RcsB
685 and GadE. Nucleic acids research. 2010;38(11):3546-54.
686 35. Pannen D, Fabisch M, Gausling L, Schnetz K. Interaction of the RcsB Response
687 Regulator with Auxiliary Transcription Regulators in Escherichia coli. The Journal of
688 biological chemistry. 2016;291(5):2357-70.
689 36. Stratmann T, Pul U, Wurm R, Wagner R, Schnetz K. RcsB-BglJ activates the
690 Escherichia coli leuO gene, encoding an H-NS antagonist and pleiotropic regulator of
691 virulence determinants. Molecular microbiology. 2012;83(6):1109-23.
692 37. Kuhne C, Singer HM, Grabisch E, Codutti L, Carlomagno T, Scrima A, et al. RflM
693 mediates target specificity of the RcsCDB phosphorelay system for transcriptional
694 repression of flagellar synthesis in Salmonella enterica. Molecular microbiology.
695 2016;101(5):841-55.
696 38. Nassif X, Honore N, Vasselon T, Cole ST, Sansonetti PJ. Positive control of
697 colanic acid synthesis in Escherichia coli by rmpA and rmpB, two virulence-plasmid
698 genes of Klebsiella pneumoniae. Molecular microbiology. 1989;3(10):1349-59.
699 39. Mouslim C, Latifi T, Groisman EA. Signal-dependent requirement for the co-
700 activator protein RcsA in transcription of the RcsB-regulated ugd gene. The Journal of
701 biological chemistry. 2003;278(50):50588-95.
702 40. Thao S, Chen CS, Zhu H, Escalante-Semerena JC. Nepsilon-lysine acetylation of
703 a bacterial transcription factor inhibits Its DNA-binding activity. PloS one.
704 2010;5(12):e15123.
705 41. Kuhn ML, Zemaitaitis B, Hu LI, Sahu A, Sorensen D, Minasov G, et al. Structural,
706 kinetic and proteomic characterization of acetyl phosphate-dependent bacterial
707 protein acetylation. PloS one. 2014;9(4):e94816.
708 42. Schilling B, Christensen D, Davis R, Sahu AK, Hu LI, Walker-Peddakotla A, et al.
709 Protein acetylation dynamics in response to carbon overflow in Escherichia coli.
710 Molecular microbiology. 2015;98(5):847-63.

711 43. Weinert BT, Iesmantavicius V, Wagner SA, Scholz C, Gummesson B, Beli P, et
712 al. Acetyl-phosphate is a critical determinant of lysine acetylation in E. coli. Molecular
713 cell. 2013;51(2):265-72.
714 44. Hentchel KL, Escalante-Semerena JC. Acylation of Biomolecules in
715 Prokaryotes: a Widespread Strategy for the Control of Biological Function and
716 Metabolic Stress. Microbiology and molecular biology reviews : MMBR.
717 2015;79(3):321-46.
718 45. Wolfe AJ. Bacterial protein acetylation: new discoveries unanswered
719 questions. Current genetics. 2016;62(2):335-41.
720 46. Ren J, Sang Y, Tan Y, Tao J, Ni J, Liu S, et al. Acetylation of Lysine 201 Inhibits
721 the DNA-Binding Ability of PhoP to Regulate Salmonella Virulence. PLoS pathogens.
722 2016;12(3):e1005458.
723 47. Castano-Cerezo S, Bernal V, Post H, Fuhrer T, Cappadona S, Sanchez-Diaz NC,
724 et al. Protein acetylation affects acetate metabolism, motility and acid stress response
725 in Escherichia coli. Molecular systems biology. 2014;10:762.
726 48. Datsenko KA, Wanner BL. One-step inactivation of chromosomal genes in
727 Escherichia coli K-12 using PCR products. Proceedings of the National Academy of
728 Sciences of the United States of America. 2000;97(12):6640-5.
729 49. Baba T, Ara T, Hasegawa M, Takai Y, Okumura Y, Baba M, et al. Construction of
730 Escherichia coli K-12 in-frame, single-gene knockout mutants: the Keio collection.
731 Molecular systems biology. 2006;2:2006 0008.
732 50. Dieckman L, Gu M, Stols L, Donnelly MI, Collart FR. High throughput methods
733 for gene cloning and expression. Protein expression and purification. 2002;25(1):1-7.
734 51. Kitagawa M, Ara T, Arifuzzaman M, Ioka-Nakamichi T, Inamoto E, Toyonaga H,
735 et al. Complete set of ORF clones of Escherichia coli ASKA library (a complete set of E.
736 coli K-12 ORF archive): unique resources for biological research. DNA research : an
737 international journal for rapid publication of reports on genes and genomes.
738 2005;12(5):291-9.
739 52. Stols L, Gu M, Dieckman L, Raffen R, Collart FR, Donnelly MI. A new vector for
740 high-throughput, ligation-independent cloning encoding a tobacco etch virus
741 protease cleavage site. Protein expression and purification. 2002;25(1):8-15.
742 53. Eschenfeldt WH, Makowska-Grzyska M, Stols L, Donnelly MI, Jedrzejczak R,
743 Joachimiak A. New LIC vectors for production of proteins from genes containing rare
744 codons. J Struct Funct Genomics. 2013;14(4):135-44.
745 54. Kuhn ML, Majorek KA, Minor W, Anderson WF. Broad-substrate screen as a
746 tool to identify substrates for bacterial Gcn5-related N-acetyltransferases with
747 unknown substrate specificity. Protein science : a publication of the Protein Society.
748 2013;22(2):222-30.
749 55. Majorek KA, Kuhn ML, Chruszcz M, Anderson WF, Minor W. Structural,
750 functional, and inhibition studies of a Gcn5-related N-acetyltransferase (GNAT)
751 superfamily protein PA4794: a new C-terminal lysine protein acetyltransferase from
752 pseudomonas aeruginosa. The Journal of biological chemistry. 2013;288(42):30223-
753 35.
754 56. Majorek KA, Osinski T, Tran DT, Revilla A, Anderson WF, Minor W, et al. Insight
755 into the 3D structure and substrate specificity of previously uncharacterized GNAT

superfamily acetyltransferases from pathogenic bacteria. Biochim Biophys Acta. 2017;1865(1):55-64.
57. Vetting MW, Bareich DC, Yu M, Blanchard JS. Crystal structure of RimI from Salmonella typhimurium LT2, the GNAT responsible for N(alpha)-acetylation of ribosomal protein S18. Protein Sci. 2008;17(10):1781-90.
58. Stout V, Gottesman S. RcsB and RcsC: a two-component regulator of capsule synthesis in Escherichia coli. Journal of bacteriology. 1990;172(2):659-69.
59. Altschul SF, Madden TL, Schaffer AA, Zhang J, Zhang Z, Miller W, et al. Gapped BLAST and PSI-BLAST: a new generation of protein database search programs. Nucleic acids research. 1997;25(17):3389-402.
60. Brill JA, Quinlan-Walshe C, Gottesman S. Fine-structure mapping and identification of two regulators of capsule synthesis in Escherichia coli K-12. Journal of bacteriology. 1988;170(6):2599-611.
61. Majdalani N, Heck M, Stout V, Gottesman S. Role of RcsF in signaling to the Rcs phosphorelay pathway in Escherichia coli. Journal of bacteriology. 2005;187(19):6770-8.
62. Pruss BM, Besemann C, Denton A, Wolfe AJ. A complex transcription network controls the early stages of biofilm development by Escherichia coli. Journal of bacteriology. 2006;188(11):3731-9.
63. Laubacher ME, Ades SE. The Rcs phosphorelay is a cell envelope stress response activated by peptidoglycan stress and contributes to intrinsic antibiotic resistance. Journal of bacteriology. 2008;190(6):2065-74.
64. Richter L, Johnston A, Lam A. The Rcs Phosphorelay System and RcsB Regulated rprA Contribute to Intrinsic Antibiotic Resistance in Escherichia coli Exposed to Antibiotics Targeting the Cell Wall. J Exper Microbiol and Immunol. 2016;2:42-8.
65. Chattopadhyay MK, Keembiyehetty CN, Chen W, Tabor H. Polyamines Stimulate the Level of the sigma38 Subunit (RpoS) of Escherichia coli RNA Polymerase, Resulting in the Induction of the Glutamate Decarboxylase-dependent Acid Response System via the gadE Regulon. The Journal of biological chemistry. 2015;290(29):17809-21.
66. Castanie-Cornet MP, Treffandier H, Francez-Charlot A, Gutierrez C, Cam K. The glutamate-dependent acid resistance system in Escherichia coli: essential and dual role of the His-Asp phosphorelay RcsCDB/AF. Microbiology. 2007;153(Pt 1):238-46.
67. Carper SW, Willis DG, Manning KA, Gerner EW. Spermidine acetylation in response to a variety of stresses in Escherichia coli. The Journal of biological chemistry. 1991;266(19):12439-41.
68. Silhavy TJ, Berman, M. L., and Enquist, L. W. Experiments with gene fusions. Cold Spring Harbor, NY: Cold Spring Harbor Laboratory; 1984.
69. Powell BS, Rivas MP, Court DL, Nakamura Y, Turnbough CL, Jr. Rapid confirmation of single copy lambda prophage integration by PCR. Nucleic acids research. 1994;22(25):5765-6.
70. Hanahan D. Studies on transformation of Escherichia coli with plasmids. Journal of molecular biology. 1983;166(4):557-80.
71. Chung CT, Niemela SL, Miller RH. One-step preparation of competent Escherichia coli: transformation and storage of bacterial cells in the same solution.

802 Proceedings of the National Academy of Sciences of the United States of America.
803 1989;86(7):2172-5.
804 72. Anderson WFE. Structural Genomics and Drug Discovery. Methods and
805 Protocols. 1 ed: Humana Press; 2014. 344 p.
806 73. Kwon K, Peterson SN. High-throughput cloning for biophysical applications.
807 Methods in molecular biology. 2014;1140:61-74.
808 74. Makowska-Grzyska M, Kim Y, Maltseva N, Li H, Zhou M, Joachimiak G, et al.
809 Protein production for structural genomics using E. coli expression. Methods in
810 molecular biology. 2014;1140:89-105.
811 75. Kuhn ML, Majorek KA, Minor W, Anderson WF. Broad-substrate screen as a
812 tool to identify substrates for bacterial Gcn5-related N-acetyltransferases with
813 unknown substrate specificity. Protein Science. 2013;22(2):222-30.
814

815

Supporting information

S1 Fig. The effect of spermidine on rprA in the absence of SpeE.

The *speE* mutant was transformed with either the VC or pSpeG and grown in TB7 supplemented with 50 μM IPTG and 0, 1.5, 2.5, or 5 mM spermidine. Growth and *rprA* promoter activity was measured over time. Each data point is an average of duplicate biological replicates and standard deviations.

S2 Fig. Affinity analysis of RcsB binding to SpeG.

(A) The maximum responses in the SPR sensograms for the first dilution series of RcsB C-terminal domain in the absence of spermidine are plotted against the analyte concentration. (B and C) The SPR sensograms for dilution series of RcsB full-length and its C-terminal domain after exposure to spermidine. The RcsB full-length or RcsB C-terminal domain protein was injected in five dilution series with the following concentrations: 21, 42, 53, 63 and 74 μM (B) or 23, 45, 91, 114, and 136 μM (C). The fitted data are shown in black.

S3 Fig. Phylogenetic tree of LuxR/FixJ DNA-binding domain of transcriptional regulators.

Phylogenetic tree was created in ClustalW2 server (http://www.ebi.ac.uk/Tools/msa/clustalw2). A list of 58 representatives of the conserved LuxR/FixJ DNA-binding domains was generated in NCBI server http://www.ncbi.nlm.nih.gov/Structure/cdd) and includes DNA-binding domains of following transcriptional factors: RcsB from *Escherichia coli* (RcsB-Es_co) [GI:353570681], RcsB from *Erwinia amylovora* (RcsB-Er_am) [GI:33357861], YjjQ from *E. coli* (YjjQ-Es_co) [GI:83288197], BglJ from *E. coli* (BglJ-Es_co)

839 [GI:3915634], YahA from *E. coli* (YahA-Es_co) [GI:2506596], YuaB from *E. coli*
840 (YuaB-Es_co) [GI:81783897], DctR from *E. coli* (DctR-Es_co) [GI:57012697],
841 RcsA from *E. coli* (RcsA-Es_co) [GI:60393000], EntR from *Citrobacter freundii*
842 (EntR-Ci_fr) [GI:6015049], FimW from *Salmonella enterica* (FimW-Sa_en)
843 [GI:585140], LuxR from *Bacteroides thetaiotoamicron* (LuxR-Ba_th)
844 [GI:171849138], YgeK from *E. coli* (YgeK-Es_co) [GI:20140955], UhpA from *E. coli*
845 (UhpA-Es_co) [GI:84029412], UvrY from *E. coli* (UvrY-Es_co) [GI:83288180],
846 PA0034 from *Pseudomonas aeruginosa* (PA0034-Ps_ae) [GI:13959718], BvgA
847 from *Bordetella pertussis* (BvgA-Bo_pe) [GI:61219948], FimZ from *E. coli* (FimZ-
848 Es_co) [GI:84028128], EvgA from *E. coli* (EvgA-Es_co) [GI:82581667], FixJ from
849 *Sinorhizobium meliloti* (FixJ-Si_me) [GI:159163516], StyR from *P. fluorescens*
850 (StyR-Ps_fl) [GI:78100993], NodW from *Bradyrhizobium diazoefficiens* (NodW-
851 Br_di) [GI:128495], Ycf29 from *Porphyra purpurea* (Ycf29-Po_pu) [GI:1723332],
852 Ycf29 from *Cyanophora paradoxa* (Ycf29-Cy_pa) [GI:1351750], NarL from *E. coli*
853 (NarL-Es_co) [GI:24158735], NarP from *E. coli* (NarP-Es_co) [GI:400374], GerE
854 from *Bacillus subtilis* (GerE-Ba_su) [GI:13786948], VraR from *Staphylococcus*
855 *aureus* (VraR-St_au) [GI:166007196], LiaR from *B. subtilis* (LiaR-Ba_su)
856 [GI:68051995], DegU from *B. subtilis* (DegU-Ba_su) [GI:118438], YxjL from *B.*
857 *subtilis* (YxjL-Ba_su) [GI:20141933], YhjB from *E. coli* (YhjB-Es_co) [GI:586682],
858 CsgD from *E. coli* (CsgD-Es_co) [GI:1706166], MoaR from *Enterobacter*
859 *aerogenes* (MoaR-En_ae) [GI:1709068], MalT from *E. coli* (MalT-Es_co)
860 [GI:189028606], SgaR from *Hyphomicrobium methylovorum* (SgaR-Hy_me)
861 [GI:6094276], Rv08090c from *Mycobacterium tuberculosis* (Rv08090c-My_tu)

862 [GI:6137301], AgmR from *P. aeruginosa* (AgmR-Ps_ae) [GI:121420], AlkS from *P.*
863 *oleovorans* (AlkS-Ps_ol) [GI:6226550], ComA from *B. subtilis* (ComA-Ba_su)
864 [GI:116903], YdfI from *B. subtilis* (YdfI-Ba_su) [GI:68566110], ExeN from
865 *Aeromonas salmonicida* (ExeN-Ae_sa) [GI:1175862], LuxR from *Aliivibrio fischeri*
866 (LuxR-Al_fi) [GI:462556], VanR from *Vibrio anguillarum* (VanR-Vi_an)
867 [GI:9297072], SolR from *Ralstonia solanacearum* (SolR-Ra_so) [GI:9297032],
868 AhyR from *Aeromonas hydrophila* (AhyR-Ae_hy) [GI:61218504], LasR from *P.*
869 *aeruginosa* (LasR-Ps_ae) [GI:125980], Y4HQ from *Sinorhizobium fredii* (Y4HQ-
870 Si_fr) [GI:2495427], SdiA from *E. coli* (SdiA-Es_co) [GI:2506570], PhzR from *P.*
871 *fluorescens* (PhzR-Ps_fl) [GI:2495423], CarR from *Pectobacterium carotovorum*
872 (CarR-Pe_ca) [GI:2495418], YenR from *Yersinia enterocolitica* (YenR-Ye_en)
873 [GI:1723596], RhiR from *Rhizobium leguminosarum* (RhiR-Rh_le) [GI:417645],
874 TraR from *S. fredii* (TraR-Si_fr) [GI:158429605], MoxX from *Paracoccus*
875 *denitrifican* (MoxX-Pa_de) [GI:266552], BrpA from *Streptomyces hygroscopicus*
876 (BrpA-St_hy) [GI:231653], RaiR from *Rhizobium etli* (RaiR-Rh_et) [GI:9297035],
877 TraR from *Agrobacterium tumefaciens* (TraR-Ag_tu) GI:23200109 and TraJ from
878 *E. coli* (TraJ-Es_co) [GI:464931].

879 **S4 Fig. SPR analysis of SpeG and RcsA interaction.**

880 The SPR sensograms of SpeG and transcription regulator RcsA. The RcsA protein
881 was injected in four dilution series. Duplicate measurements for each
882 concentration indicated above SPR sensograms were performed.

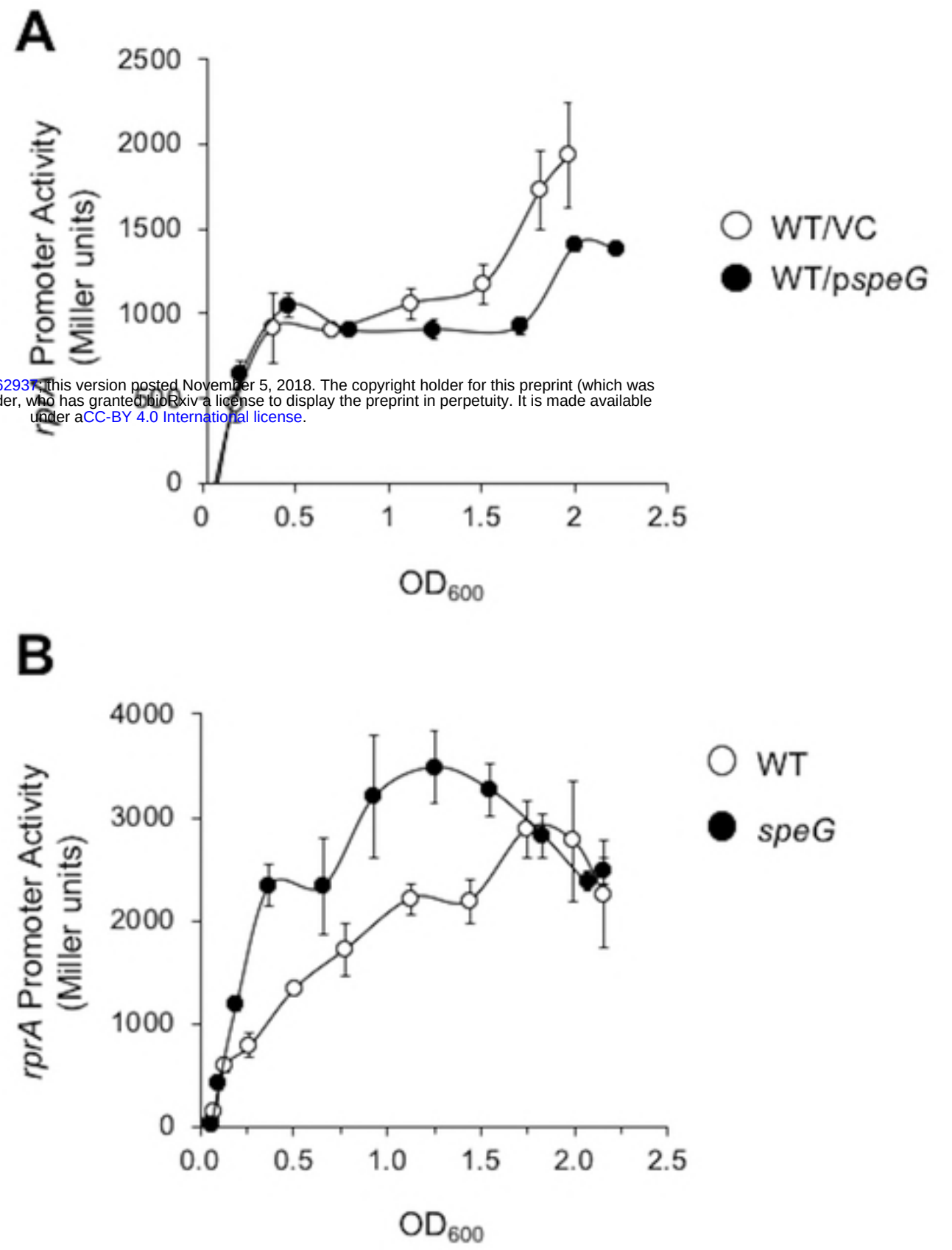

Fig1

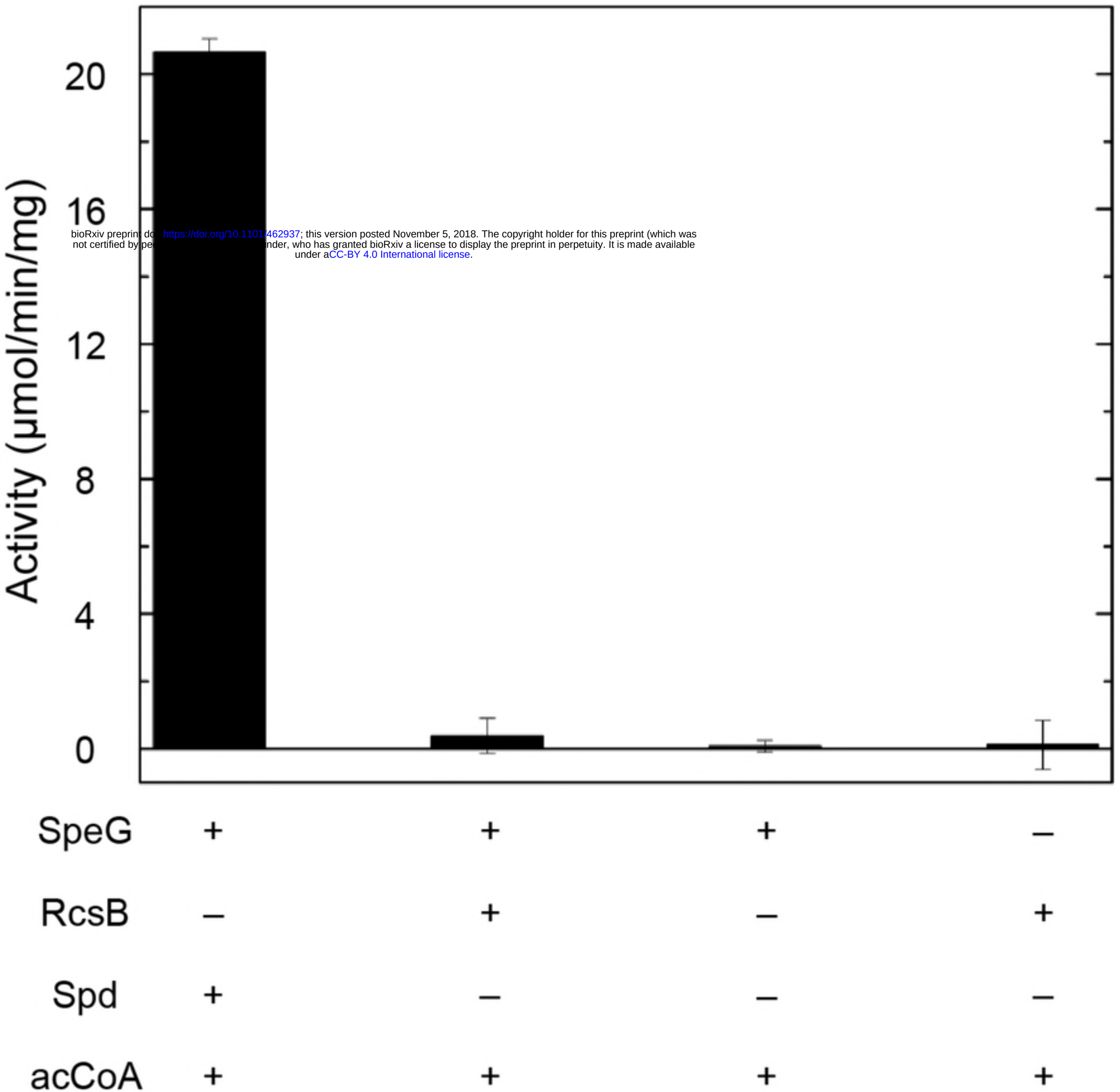

Fig2

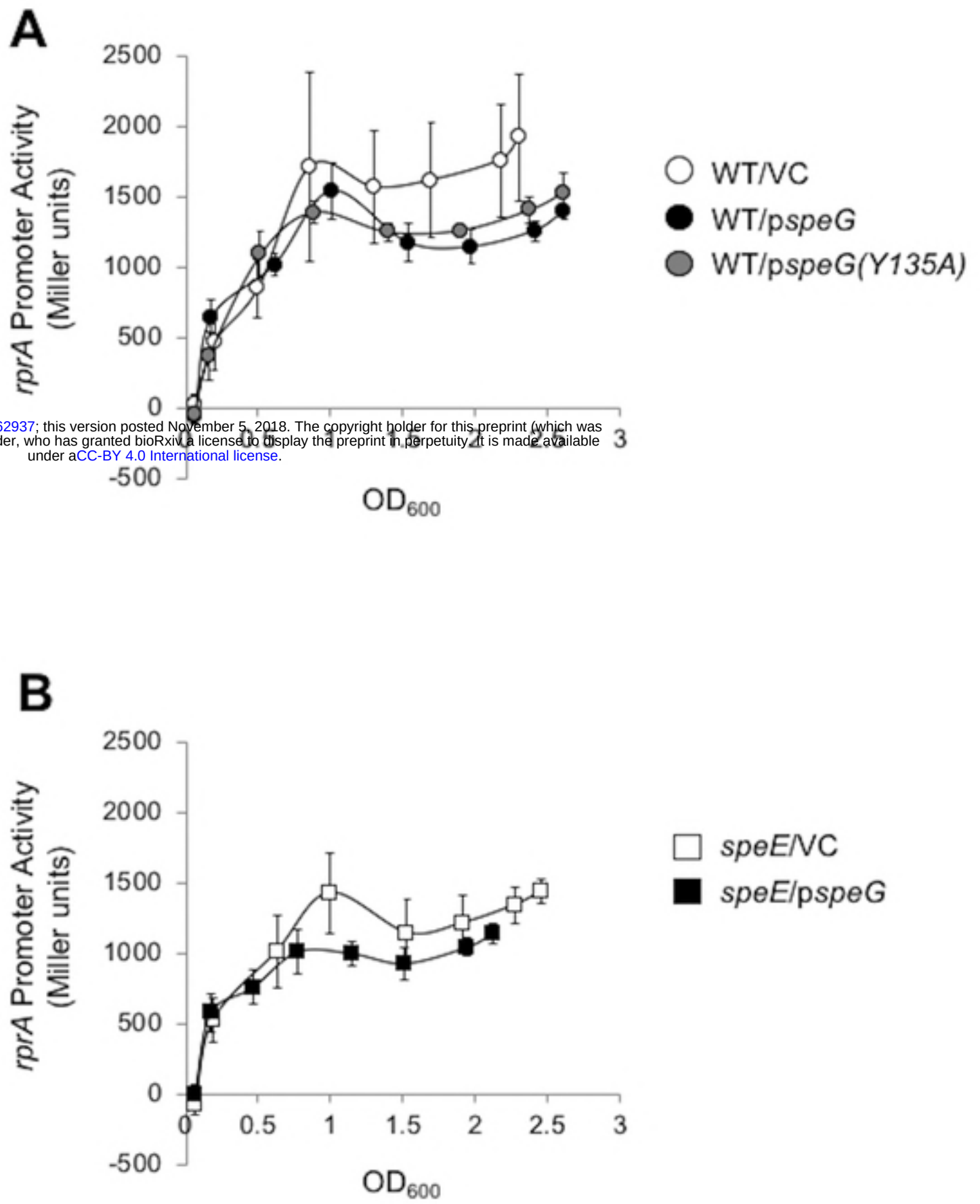

Fig3

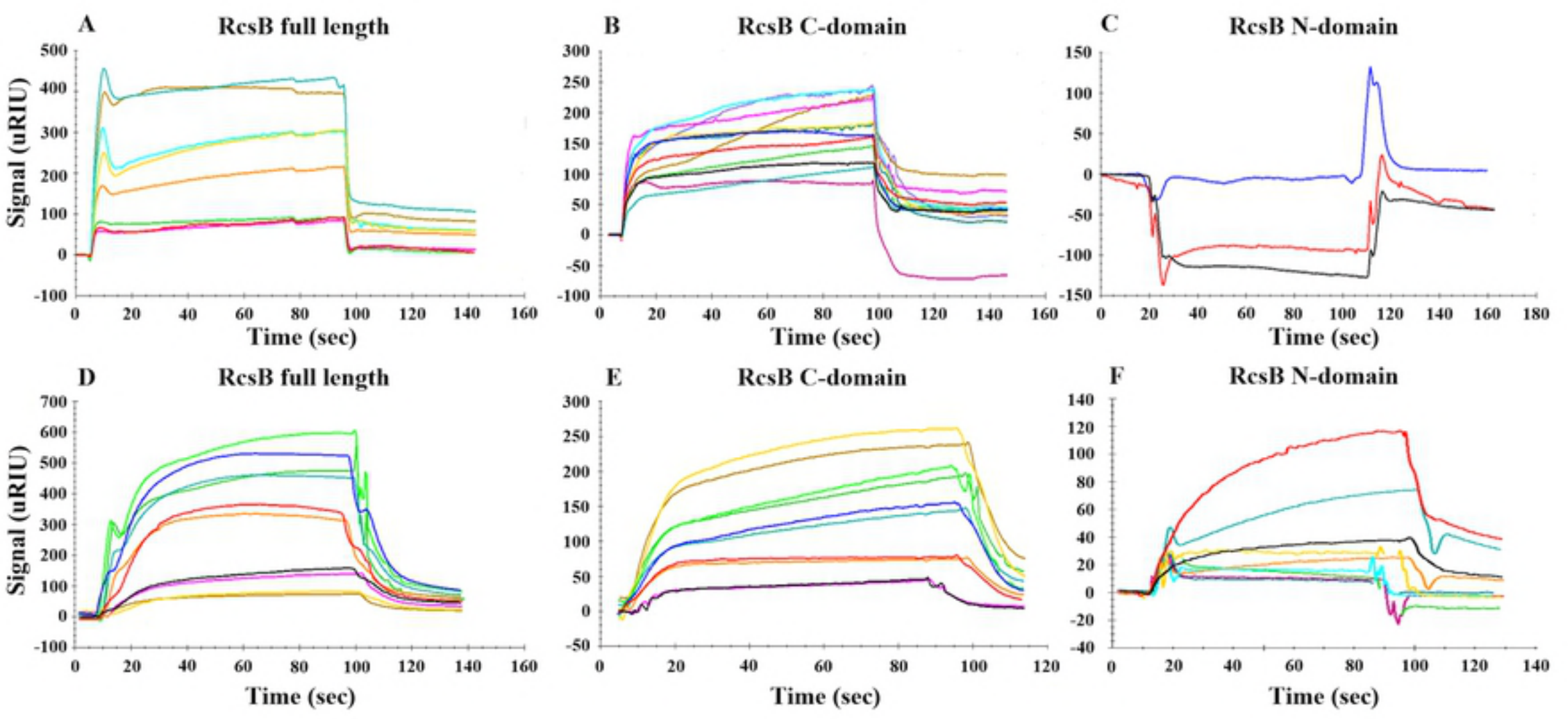
A
RcsB full length
B
RcsB C-domain
C
RcsB N-domain
D
RcsB full length
E
RcsB C-domain
F
RcsB N-domain
Signal (uRIU)
Time (sec)

Fig4

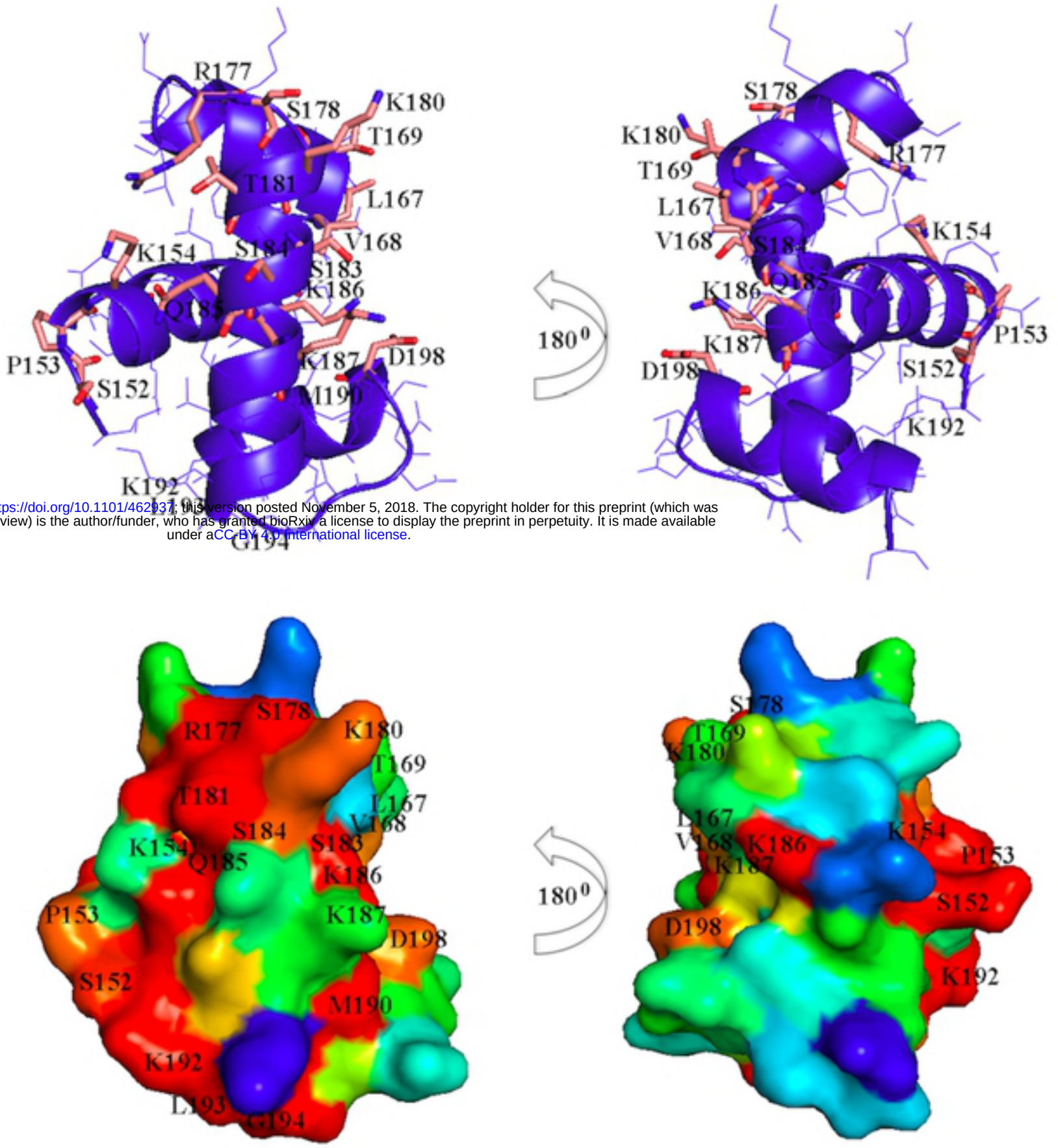

Fig5